Anales de Química Int. Ed. (1997) 93:385-393

ORIGINAL PAPER

Ana A. Palacios
Pere Alemany
Santiago Alvarez
Roald Hoffmann

Electronic structure and bonding in $BaNi_2P_4$

Received 8 April 1997
Accepted 22 April 1997

A. A. Palacios · P. Alemany · S. Alvarez
Departament de Química Inorgànica
and Departament de Química Física
Universitat de Barcelona
Diagonal 647
E-08028 Barcelona, Spain

Roald Hoffmann (✉)
Department of Chemistry
and Materials Science Center
Cornell University
Ithaca, NY 14853-1301, USA
Fax: 1-607-2555707

Abstract The electronic structures of the $(Ni_2P_4)^{2-}$ subnet of α- and β-$BaNi_2P_4$ have been investigated by means of electronic band structure calculations using the semiempirical extended Hückel tight-binding method. Molecular and chain models of the $(Ni_2P_4)^{2-}$ subnet comprising Ni_2P_2 rings have also been analyzed. Although the electronic structure for the solid is more complicated than those of the molecular and one-dimensional models, the use of the Framework Electron Counting (FEC) rules based on a molecular orbital analysis of related molecules is useful for the rationalization of the chemical bonding in the solid. The basic feature of this system is a three-dimensional network of edge-sharing NiP_4 tetrahedra, linked through P_4 squares. There are less than eight valence electrons in each Ni_2P_2 ring; different Ni···Ni contacts in the nonequivalent rings can be rationalized from this electron-deficient filling of the framework orbitals. While a simple one-dimensional model suggests a Peierls distortion as the origin of the observed phase transition in $BaNi_2P_4$, a detailed look shows that this mechanism is not operative in this metallic compound.

Key words Electronic structure · Transition-metal phosphides · Chemical bonding

Resumen La estructura electrónica de la red aniónica $(Ni_2P_4)^{2-}$, presente en las estructuras α- y β-$BaNi_2P_4$, ha sido estudiada mediante cálculos de bandas, usando el método semiempírico "extended Hückel tight-binding". También se han analizado modelos moleculares y en cadena de la subred $(Ni_2P_4)^{2-}$ que contienen anillos Ni_2P_2. Aunque la estructura electrónica del sólido es más complicada que la de los modelos, el cálculo del número de electrones del esqueleto (Framework Electron Counting, FEC), basado en un análisis de orbitales moleculares de moléculas relacionadas, es útil para la comprensión del enlace químico en el sólido. La característica principal de este sistema es la red tridimensional de tetraedros NiP_4 que comparten aristas, conectados a través de anillos cuadrados P_4. En cada anillo Ni_2P_2 hay menos de ocho electrones de valencia, y la existencia de diferentes contactos Ni···Ni en los anillos no-equivalentes pueden ser atribuídos a esta ocupación deficiente en electrones de los orbitales del esqueleto. Aunque un simple modelo monodimensional sugiere una distorsión de Peierls como el origen de la transición de fase observada en $BaNi_2P_4$, un análisis más detallado muestra que este mecanismo no es operativo en dicho compuesto metálico.

Introduction

At temperatures over 100°C, $BaNi_2P_4$ crystallizes in a tetragonal structure [1] formed by condensation of relatively large Ni_8P_{16} cages each of which contains a single barium atom in its interior (Fig. 1). The same crystal structure has also been reported [2] for $BaPd_2P_4$. An alternative view of this structure is to consider the phosphorus-nickel sublattice as being composed of linear chains (**1a**) of edge-sharing NiP_4 tetrahedra running along the [001] direction in the

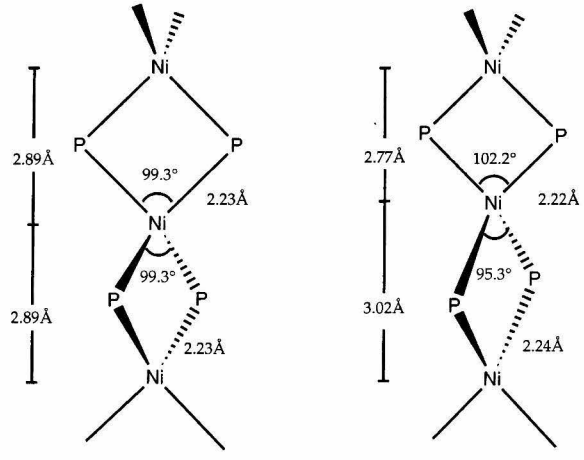

1a **1b**

crystal. These chains are arranged in such a way that four phosphorus atoms belonging to four distinct chains form square P_4 rings with short P-P distances (2.23Å) that can be identified as single P-P bonds. Similar square P_4 rings have also been found in binary MP_3 transition-metal phosphides with the skutterudite structure and for the related RM_4P_{12} filled skutterudites, and have been of theoretical interest to us [3, 4].

On lowering the temperature, the tetragonal α-$BaNi_2P_4$ phase undergoes a gradual transition to a lower symmetry, orthorhombic β-$BaNi_2P_4$ phase. The structure of this low temperature phase is essentially the same as that found for α-$BaNi_2P_4$, its main difference being that now the NiP_4 tetrahedra are distorted, resulting in chains of edge-sharing tetrahedra with alternating Ni-Ni distances (**1b**). As a side effect, the P_4 rings are now slightly compressed, with practically the same P-P distance as in the high temperature phase.

In this contribution we will use the semiempirical extended Hückel method (see Appendix for computational details) to analyze the bonding in the $(Ni_2P_4)^{2-}$ subnet of $BaNi_2P_4$. Our main aim is to look for simple electron counting rules that explain the presence of short Ni-Ni distances across the Ni_2P_2 rings in the low temperature phase. The elegant synthetic work reporting the original structure and its deformations was accompanied by a theoretical analysis, in fact using a methodology similar to ours. However, as we will see, there are certain problems in the reported theoretical modeling. This and the inherently intriguing structure has led us to undertake an independent study of the electronic structure of this material.

Framework Electron Counting

The nickel atoms in both phases of $BaNi_2P_4$ have tetrahedral environments. By sharing the vertices (and edges) of the NiP_4 tetrahedra one can build up the chains present in these two structures. An alternative view of these chains is as an array of alternating, mutually perpendicular Ni_2P_2 diamonds. Such basic M_2X_2 building blocks are very common in organometallic chemistry; there are large families of

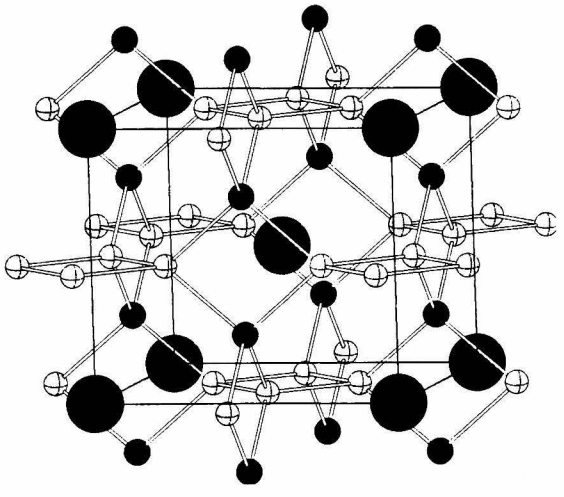

Fig. 1 Crystal structure of α-$BaNi_2P_4$. Small black circles represent Ni atoms; small white circles, P atoms, and large gray circles, Ba atoms

$L_4M_2(\mu\text{-}XR_n)_2$ molecules with a wide range of metal-metal separations across the ring. A workable rationalization of the different bonding situations encountered in these compounds is provided by the Framework Electron Counting (FEC) rules [5, 6]. These rules, based on a molecular orbital analysis of the σ-type bonds in the diamond-shaped M_2X_2 framework, provide a simple tool to predict the existence or absence of M···M interactions across the rings, which in turn lead to more or less squeezed diamonds.

Let us take a simple model $L_4M_2(\mu\text{-}XR_2)_2$ compound to illustrate these electron counting rules. Each XR_2 bridging ligand can contribute two orbitals to framework bonding. If we consider M to be a d^{10} metal ion (i.e., Cu^+ or Ni^0), where it is likely that we may neglect participation of d orbitals in the M_2X_2 ring bonding, the metal atom is left with two empty sp^3 orbitals available for framework bonding. The orbitals of the XR_2 and ML_n fragments interact as shown in the diagram presented in Fig. 2. Four M-X bonding orbitals and their corresponding antibonding counterparts result. If each bridging XR_2 ligand is able to contribute four electrons to the framework, as in the case of PH_2^-, the four M-X bonding framework orbitals will be totally occupied and the framework electron count (FEC) is eight. If we analyze more carefully the shape of the four M-X bonding framework orbitals (**2a-d**), we may easily convince ourselves that no net M···M or X···X bonding interactions can be expected. The FEC = 8 case corresponds thus to the canonical situation of four localized M-X bonds, as found in cyclobutane.

a **b** **c** **d**

2

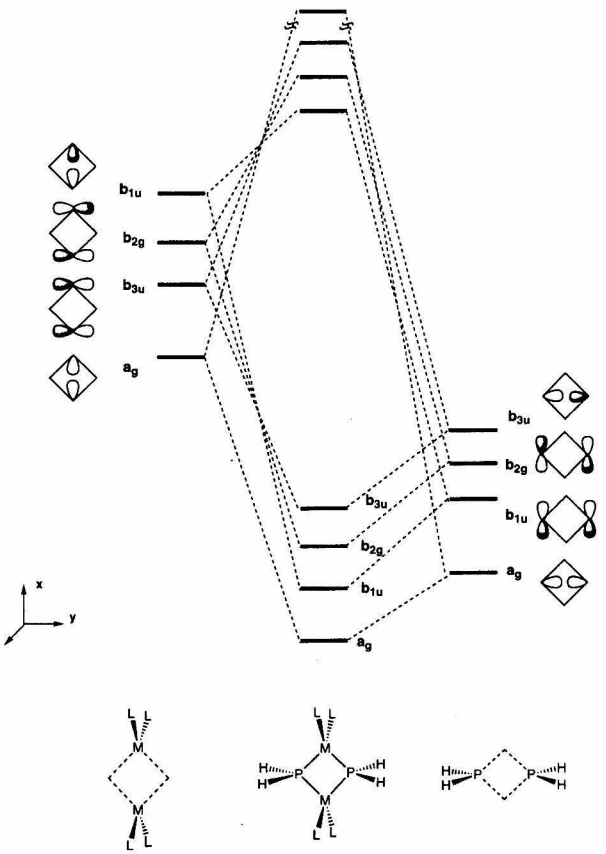

Fig. 2 Qualitative interaction diagram for the framework orbitals of $[L_4M_2(\mu\text{-}XR_2)_2]$

Another interesting situation occurs when we consider XR_3 ligands, such as phosphine. In this case each bridging ligand can only contribute to framework bonding through its lone pair or radical σ-orbital. The net result is that we only will have two M-X bonding framework orbitals (a_g and b_{3u}) and two non-bonding, metal centered orbitals (b_{1u} and b_{2g}). Filling the framework orbitals for this electron count (FEC = 4), leads to a net attractive M···M interaction across the ring since both orbitals are M···M bonding. This situation, four atoms sharing four electrons with delocalized bonding in the ring, is the same as in the archetypal diborane molecule.

An intermediate case is provided by $L_4M_2(\mu\text{-}XR_2)_2$ with FEC = 6. By removing two electrons from the four bonding framework orbitals a net M···M or X···X interaction can be created. For this case two different minima appear in a plot of the energy as a function of the X-M-X angle, corresponding to geometries with either short M···M or X···X distances. For a more detailed account of the application of the framework electron counting rules to a large set of organometallic compounds, the reader is referred to the original formulation of these rules [5, 6].

Let us now try to apply the FEC rules to the basic Ni_2P_2 building units in $BaNi_2P_4$. A reasonable molecular model for these units can be obtained by taking two edge-sharing NiP_4 tetrahedra and saturating all the dangling bonds with hydrogen atoms to obtain the $(PH_3)_4Ni_2(\mu\text{-}PH_2)_2$ compound

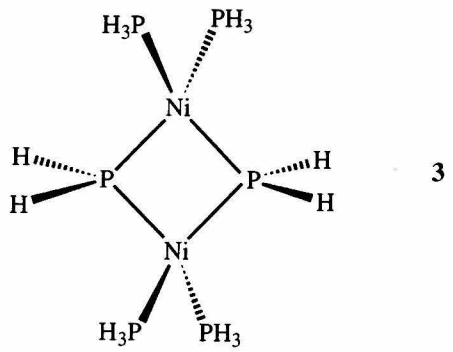

3

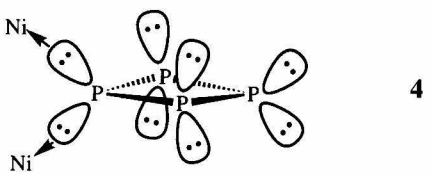

4

shown in **3**. That fixes the periphery of the model, but how many electrons should we have in the ring to represent properly the bonding situation found in $BaNi_2P_4$? If we consider that the barium atoms act merely as electron donors we are led to a -2 charge on the Ni_2P_4 subnet. One way to reach the appropriate electron count is to first complete the octet at each four-membered ring P. That would give a P_4^{4-} (as in **4**), or a $Ni_2P_4^{4-}$. Of course we have two electrons less, i.e. $Ni_2P_4^{2-}$, indicating that each P is on average half electron short of an octet (or there is a half electron hole in the Ni 3d block, unlikely because of the tetrahedral coordination of typical four-coordinated Ni^0). The result is that in the Ni_2P_2 ring the FEC is not 8, but 7. The appropriate model in which we replace the "terminal" P on each Ni by PH_3 and the bridging P by PH_2 is $[Ni_2(PH_3)_4(PH_2)_2]^{-1}$.

A plot of the energy as a function of the P-Ni-P angle (Fig. 3) has a single minimum at 98°, a value very close to that found in α-$BaNi_2P_4$ (99.3°). The intermediate situation

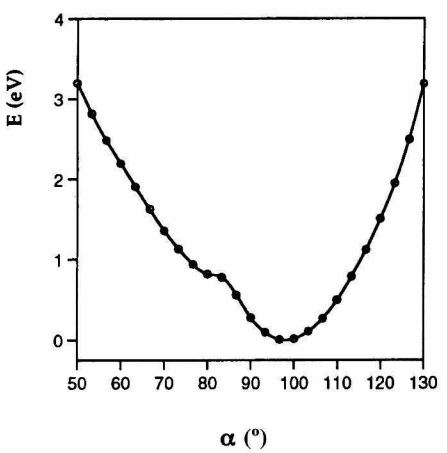

Fig. 3 One electron relative energy curve for the ring squeezing of the $[(PH_3)_4Ni_2(\mu\text{-}PH_2)_2]^-$ model molecule with FEC = 7

between FEC = 6 (double minimum) and FEC = 8 (single minimum, no interactions across the ring) is evident in the hump that is found in the energy curve for angles close to 80°, a feature which is a typical sign of level crossing. Analysis of bonding in the Ni_2P_2 rings (see Table 1) shows that, as expected, framework Ni-P bonding is weakened upon removing electrons, while weak Ni···Ni bonding interactions across the ring are only expected for the FEC = 6 case. The Ni···Ni distance of 2.92Å found for the FEC = 7 case is significantly longer than twice the metallic radius of nickel. This, together with the negative Ni···Ni overlap population computed in this case, indicates that there is no Ni···Ni bonding in the present FEC = 7 case.

Electronic structure of $BaNi_2P_4$

The preceding discussion sets the framework for an analysis of the fascinating network in $BaNi_2P_4$. In this section we will turn our attention to the specific aspects of bonding in the two crystalline phases of $BaNi_2P_4$. We will proceed in two steps, starting with the electronic structure of a single chain of edge-sharing NiP_4 tetrahedra. After analyzing framework bonding for this relatively simple model, we will move to a more precise model for the solid phases, the 3D $(Ni_2P_4)^{2-}$ subnet.

Framework bonding in a chain of edge sharing tetrahedra

To identify the relevant bonding features in the complex solid state structure of $BaNi_2P_4$ consider the simple chain of edge-sharing tetrahedra shown in **5**. The dangling bonds on the bridging phosphorus atoms have been saturated by hydrogen atoms. Again the electron count for the extended polymer is not obvious, but needs to be reasoned out carefully. The essential feature of the $(Ni_2P_4)^{2-}$ system in the full three-dimensional system is that each P bridging nickel atoms is not a closed octet (P^{3-} or PH_2^-), but rather is one half of an electron short per PH_2^-. To get the same number of electrons per Ni_2P_2 ring as in the solid state compound we have to assign in this one-dimensional model to each unit cell a 2- charge, i.e. $[Ni_2(PH_2)_4]^{2-}$. The plot of the total energy of the chain as a function of the P-Ni-P angle (not

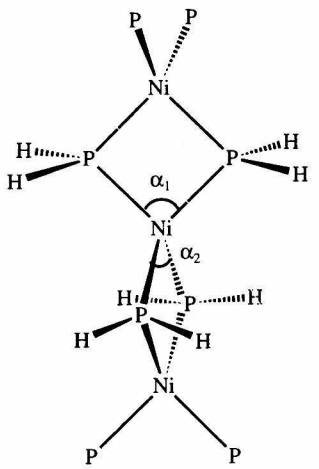

5

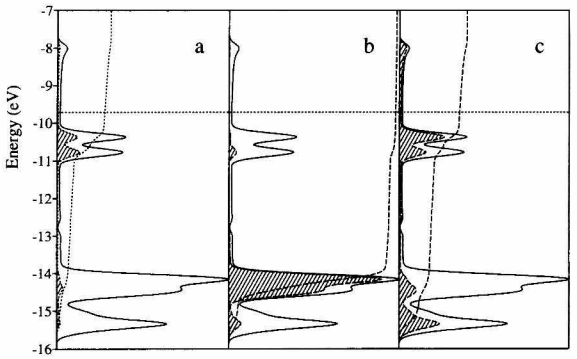

Fig. 4 Calculated density of states (DOS) curves for the $[Ni_2(PH_2)_4]^{2-}$ chain. The shaded areas correspond to the contribution of the 4s and 4p orbitals of the Ni atoms (a), the 3d orbitals of Ni atoms (b), and the P atoms (c) to the total DOS. The dotted curve indicates the integration of each contribution to the total DOS

shown) is practically identical to that found for the molecular model (Fig. 3), with a single minimum at 101.9°, close to the experimental value in α-$BaNi_2P_4$ (99.3°). For this experimental angle, both overlap populations and net charges on the P atoms are very close to the ones found for the molecular model with FEC = 7.

The analysis of the calculated density of states (DOS) curve and its atomic projections for this model structure (Fig. 4) allows us to identify three qualitatively different types of bands in the region around the Fermi level. The peak that appears between -15 and -16 eV is basically due to P-H bonding in the bridges. The projected DOS curve for the H atoms (not shown in the Figure) allows us to rule out important contributions of these atoms in the other regions of the DOS curve (except for high lying P-H antibonding bands), so that we can be confident that the atoms used for saturating the dangling bonds in our model are not introducing significant perturbations in Ni-P framework bonding.

The sharp peak at -14.5 eV is mainly due to the 3d orbitals of the Ni atoms; it is clear that our initial assumption of neutral Ni atoms with a d^{10} configuration is essentially correct. The wide band of levels stretching from -13.0 to -8.0 eV is basically built up by Ni 4s and 4p orbitals, together with important contributions from the phosphorus atoms. These levels may be identified with the framework orbitals discussed for our molecular model. A more careful analysis shows that the lowest lying framework bands, those coming from the a_g framework orbital, appear in the same region as the 3d bands of nickel.

Table 1 Ring geometry and overlap populations for the $[(PH_3)_4Ni_2(\mu\text{-}PH_2)_2]^{n-}$ model compound with different framework electron counts

	n = 2	n = 1	n = 0
FEC	8	7	6
P-Ni-P (°)	92.2	98.0	107.4
Ni-Ni (Å)	3.09	2.92	2.64
OP (Ni-P)	0.655	0.621	0.598
OP (Ni-Ni)	-0.071	-0.030	0.068

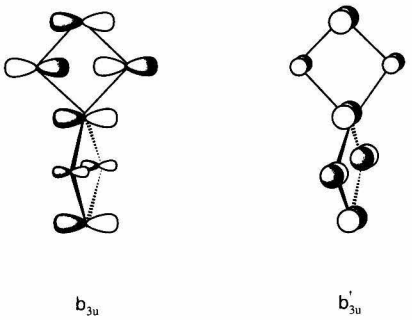

6

The band structure for the model $[Ni_2(PH_2)_4]^{2-}$ chain is shown in Fig. 5a, where the framework bands have been highlighted. The same symmetry labels that were used for the molecular model have been adopted to indicate the framework orbital from which each band is derived. Notice, however, that because of the presence of a 4_2 screw-axis relating the two $Ni_2(PH_2)_2$ rings in the unit cell, the framework orbitals of one Ni_2P_2 ring combine in the same band with π-type orbitals of the neighboring ring, as illustrated in **6** for the case of the b_{3u} band. Another consequence of the existence of a screw axis is seen in the dispersion diagram (Fig. 5a); the bands are doubled, presenting two branches that are degenerate at the edge of the Brillouin zone (Z point in Fig. 5a). In the case of the b_{3u} and b_{2g} bands, the band doubling cannot be appreciated in Fig. 5a because the two branches are degenerate along the ΓZ line. The Fermi level for this model structure is located at the point where the two b_{1u} branches meet, thus giving a half-filled framework band, which is consistent with a FEC of 7 per $Ni_2(PH_2)_2$ ring. For later discussion it is important to realize that the a_g and b_{1u} are strongly dispersed because of their σ character along the chain direction (**2**), whereas the b_{3u} and b_{2g} band show little dispersion. A study of chains of edge-sharing tetrahedra present in the $AFeS_2$ compounds (A = K, Rb or Cs) has been reported previously by Silvestre and Hoffmann [7]. However, that work focused on the partially filled metal 3d bands, which are less important in the present case in which the metal 3d bands are fully occupied (below -14 eV in Fig. 5a).

The partially filled b_{1u}-type band in this 1D model immediately suggests a potential structural distortion of the Peierls type [8, 9]. Since this band is half-filled, a unit cell doubling distortion, such as the one found in the α-$BaNi_2P_4$ to β-$BaNi_2P_4$ phase transition (**1a-b**), is in principle a good candidate for opening up a gap between the two b_{1u}-type branches. That in turn should result in a lowering of the system's total energy. The extent of the distortion can be monitored by a single parameter defined as the difference between the two P-Ni-P angles in the distorted chain, $\Delta\alpha = \alpha_1 - \alpha_2$, (**5**). The effect of the distortion on the band structure of our 1D model is shown in Fig. 5 for two different values of $\Delta\alpha$. Three important features should be noticed in these dispersion diagrams: (1) as expected, the distortion opens a gap at the Fermi level, separating the two b_{1u}-type branches; (2) the Fermi level is lowered by the distortion; (3) the

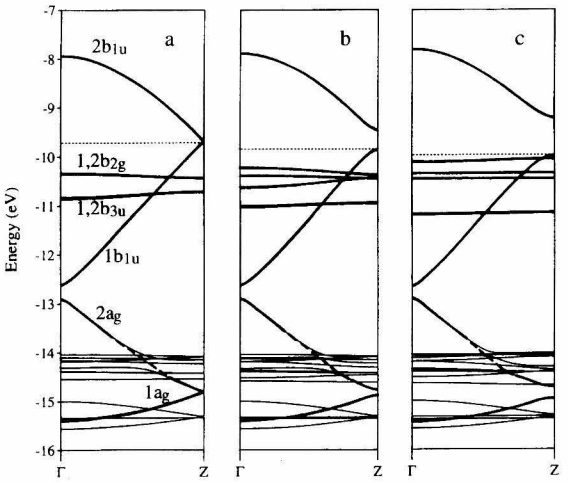

Fig. 5 Dispersion diagram for the undistorted $[Ni_2(PH_2)_4]^{2-}$ chain (a), the distorted chain with $\Delta\alpha = 10°$ (b), and the distorted chain with $\Delta\alpha = 20°$ (c). Framework bonding bands are highlighted using bold lines

degeneracy of the b_{2g}- and b_{3u}-type branches is removed by the distortion. As a consequence, one might expect that a Peierls distortion lies at the origin of the experimentally detected phase transition in $BaNi_2P_4$. A more thorough analysis will show, however, that the situation is not so simple.

If one calculates the total energy of the system, the distortion is found to be destabilizing. Why is this happening? The answer can be found in the behavior of the b_{2g}- and b_{3u}-type bands. When the degeneracy of their two branches is lifted by the distortion, the total energy of the system is increased. For these two bands the change in ring geometry favors M-P bonding in one of the two rings while weakening it in the other one (**7a-b**), resulting in the removal of degeneracy. The energy loss due to the destabilization of one branch is not compensated by the energy gain in the other branch, and the combined effect is energetically unfavorable. If one plots the contribution of each band to the energy change as a function of $\Delta\alpha$ (as

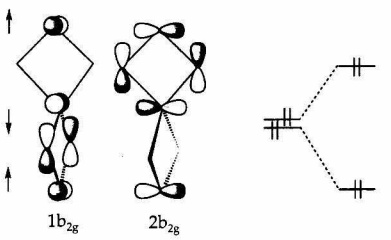

7a

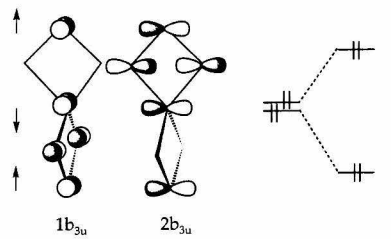

7b

Table 2 Ring geometry and overlap populations for the undistorted ($\Delta\alpha$ = 0°) and distorted ($\Delta\alpha$= 20°) $\{Ni_2(PH_2)_4\}^{2-}$ chains

	$\Delta\alpha$ = 0°	$\Delta\alpha$ = 20°	
P-Ni-P (°)	99.3	109.3	89.3
Ni-Ni (Å)	2.88	2.58	3.17
OP (Ni-P)	0.616	0.607	0.621
OP (Ni-Ni)	-0.012	0.056	-0.032

shown in Fig. 6) it is clear that the opening of the gap at the Fermi level is much smaller than the destabilization provided by the loss of degeneracy in the b_{2g}- and b_{3u}-type bands.

How does the distortion affect framework bonding in the Ni_2P_4 rings of our model? This question can be easily answered by examining the Ni-P and Ni···Ni overlap populations of the distorted chain (Table 2). The distortion localizes the occupied, stabilized b_{1u}-type branch at the rings with long Ni···Ni distances and the empty, destabilized b_{1u}-type branch at those with short Ni···Ni distances. The effect of this localization of the b_{1u}-type band is an increased Ni-P overlap population and a decreased Ni···Ni overlap population for the rings with long Ni···Ni distances. Rings with short Ni···Ni distances experience just the opposite changes in their overlap populations. From the framework bonding point of view, the distortion corresponds to converting a chain of identical FEC = 7 rings into a chain of alternating FEC = 6 (short Ni···Ni distances) and FEC = 8 (long Ni···Ni distances) Ni_2P_4 rings.

The second major problem that one finds in accepting the Peierls distortion as the origin of the phase transition in $BaNi_2P_4$ is the validity of the 1D model in representing the actual electronic structure of the $BaNi_2P_4$ crystals. In pseudo one-dimensional compounds (where Peierls-type distortions have been observed) the 3D crystal structure is built up from weakly interacting 1D units that can be, to a first approximation, considered independently. As it has already

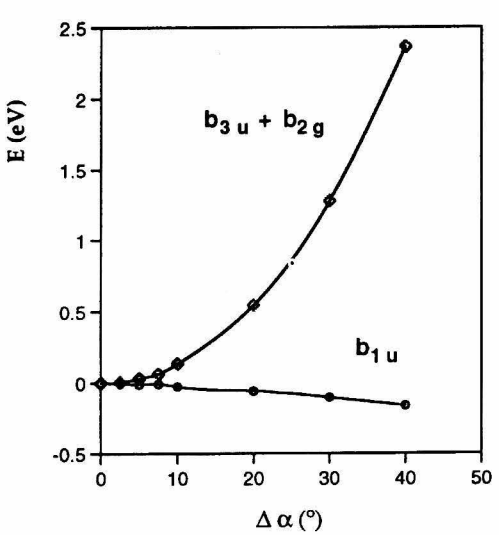

Fig. 6 Contribution of the b_{1u}, b_{3u}, and b_{2g} framework bands to the one electron energy of a $[Ni_2(PH_2)_4]^{2-}$ chain as a function of the degree of distortion $\Delta\alpha$

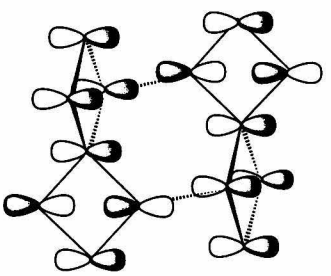

8a

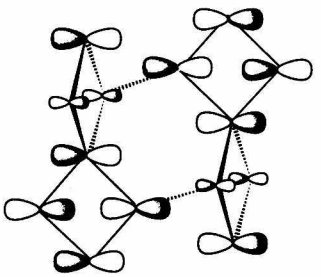

8b

been mentioned, this is not the case in $BaNi_2P_4$. In this compound the Ni_2P_4 chains are disposed in such a way that four phosphorus atoms belonging to four distinct chains form square P_4 rings with short P-P bonds, an interaction that cannot be considered as weak. A careful investigation of the band structure of the complete $Ni_2P_4^{2-}$ subnet is thus necessary before accepting (or rejecting) the Peierls' distortion hypothesis as the origin of the phase transition in $BaNi_2P_4$.

It should be noticed that electron count in our models differs fundamentally from that assumed by Keimes et al. [1]. They calculated a NiP_2^- (or $Ni_2P_4^{2-}$) polymer. While this is the electron count in the solid $Ni_2P_4^{2-}$ sublattice of $BaNi_2P_4$, the $Ni_2P_4^{2-}$ one-dimensional polymer does not take proper account of P-P bonding; it has too few electrons.

Let's be a little more specific about this. The polymer model we used was $Ni_2(PH_2)_4^{2-}$. If we strip off the H's from the phosphido groups, we must take them off as protons, otherwise octets at P are not preserved. So we would claim that an appropriate model would be $(Ni_2P_4)^{10-}$ $(H^+)_8$. It is this model which would retain the essential electronic feature of the Ni_2P_2 rings, i.e. that they have 7 framework electrons per ring. The lower dimensional model of Keimes et al. is thus quite electron poor - this may be seen by comparing the filling of electrons in their 1D polymer, which is much less than in their (and our) 3D sublattice.

Band structure of the 3D $(Ni_2P_4)^{2-}$ sublattice

As found above for the 1D model, the calculated one-electron energy of the 3D sublattice $(Ni_2P_4)^{2-}$ does not decrease upon distortion (Fig. 7). Hence, the driving force for the distortion cannot be explained at the one-electron level, although Fig. 7 suggests that distortions of a few degrees in $\Delta\alpha$ require little energy. Let us recall that the distortion found in the experimental structure of β-$BaNi_2P_4$ corresponds to $\Delta\alpha$ = 7.5°, for which we calculate a

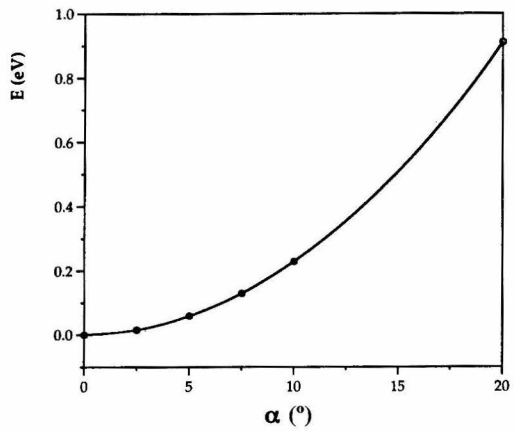

Fig. 7 One electron relative energy curve for the ring distortion (**10**) in the 3D sublattice $(Ni_2P_4)^{2-}$

destabilization of only 0.13 eV (i.e., 3.0 kcal/mol or 12.5 kJ/mol). Similar results were obtained when the Ba^{2+} ions were included in the calculation.

Even if the extended Hückel calculations do not allow us to unravel the driving force for the distortion, we can analyze those changes in the electronic structure and bonding which are related to orbital topology and symmetry and therefore well evaluated by such calculations. The band structure for the 3D $(Ni_2P_4)^{2-}$ net in the high temperature α-$BaNi_2P_4$ phase is shown in Fig. 8a. The first feature evident in this dispersion diagram is the 3D metallic character of this compound, with a complicated Fermi surface arising from the crossing of the Fermi level by multiple bands in different directions of the first Brillouin zone. Clear evidence for the 3D character of this compound can be found in the Γ-X direction, perpendicular to the Ni_2P_4 chains. Interchain coupling through the P_4 rings in this direction is responsible for the important dispersion found for the bands near the Fermi level along this symmetry line. An important difference from the one-dimensional model

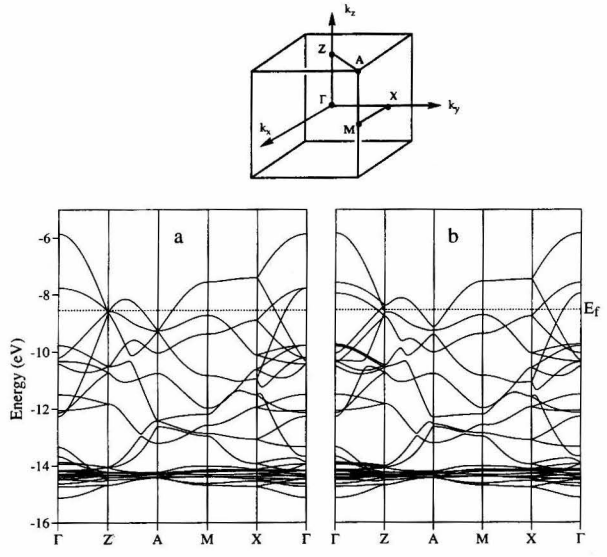

Fig. 8 Band dispersion relationships for the undistorted $(Ni_2P_4)^{2-}$ sublattice in α-$BaNi_2P_4$ (a), and for the distorted $(Ni_2P_4)^{2-}$ subnet in β-$BaNi_2P_4$ (b)

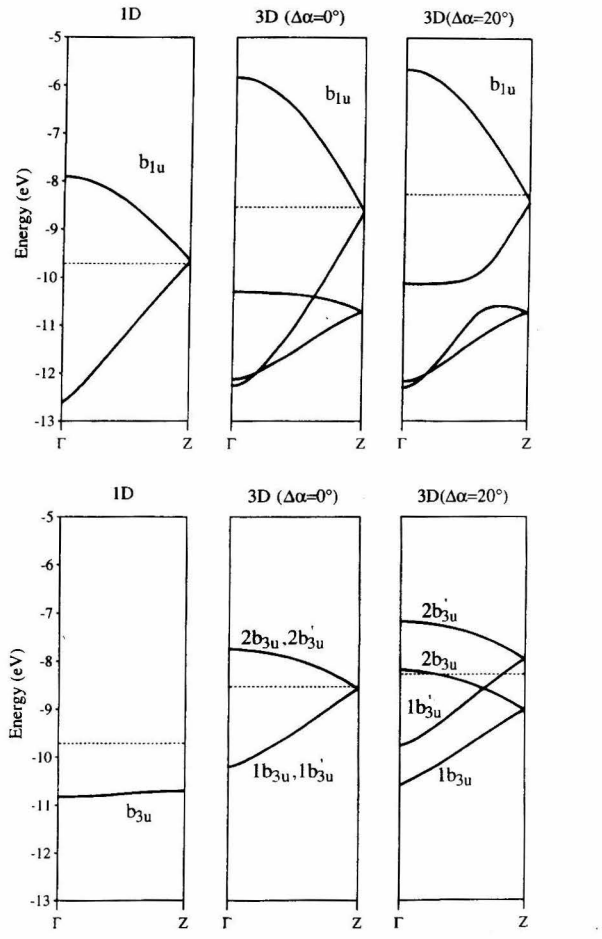

Fig. 9 Dispersion relationships in the one-dimensional model, in the 3D undistorted α-$(Ni_2P_4)^{2-}$ and distorted (Δα = 20°) $(Ni_2P_4)^{2-}$ sublattices for the b_{1u} *(top)* and b_{3u} *(bottom)* bands along theΓZ line of the Brillouin zone

studied above is that not only the b_{1u}, but also the b_{3u} band crosses the Fermi level. Let us recall that the b_{3u} orbital gave rise to a flat band in the 1D model (Fig. 5). Hence, it is interesting to analyze the differences between the band structures of the 1D model and the 3D α-structure along the chain direction (the ΓZ direction of the Brillouin zone). In Fig. 9 we have abstracted the levels corresponding to the b_{1u} and b_{3u} bands in that direction to simplify the discussion.

In order to understand the dispersion patterns of the b_{1u} and b_{3u} bands (Fig. 9) we must recall that there are two chains per unit cell and that they combine a framework orbital of one Ni_2P_2 ring with a π orbital of the neighboring ring, because of the presence of a screw axis. Hence, the number of bands is twice that found in the 1D model (Fig. 5), formed as in-phase and out-of-phase combinations of the crystal orbitals of the two chains in the unit cell. Since the chains are connected through P-P bonds of P_4 rings, one of the b_{1u} bands is stabilized, the other one destabilized as seen in Fig. 9. As for the b_{3u} bands, there are three important differences with the one-dimensional model. First, these bands appear at higher energy as a result of changing its character from σ_{PH} of the PH_2 bridging groups to σ_{PP} of the

Table 3 Ring geometry and overlap populations for the undistorted ($\Delta\alpha$ = 0°) and distorted ($\Delta\alpha$ = 20°) $[Ni_2P_4]^{2-}$ solid

	$\Delta\alpha$= 0°	$\Delta\alpha$ = 20°	
		ring **A**	ring **B**
P-Ni-P (°)	99.3	109.3	89.3
Ni-Ni (Å)	2.88	2.58	3.17
OP (Ni-P)	0.594	0.6048	0.5708
OP (Ni-Ni)	-0.033	0.0174	-0.0408
P net charge	0.64	0.57	0.70

Table 4 Atomic parameters used for the extended Hückel calculations

Atom	Orbital	Hii (eV)	ζ_i1	(c1)	ζ_i2	(c2)	Ref.
Ni	4s	-10.95	2.10				[20]
	4p	-6.27	2.10				
	3d	-14.20	5.75	(0.5493)	2.30	(0.6082)	
P	3s	-18.40	1.81				[21]
	3p	-9.80	1.45				
Ba	6s	-5.49	2.10				[22, 23]
	6p	-3.56	2.10				
H	1s	-13.60	1.30				15]

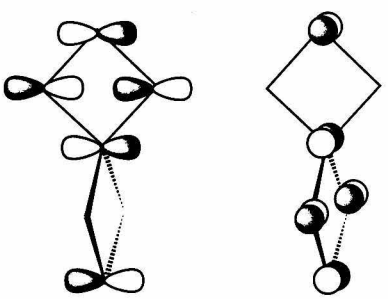

9a **9b**

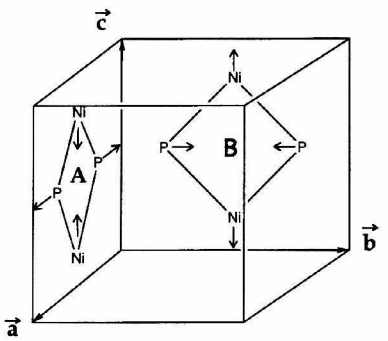

10

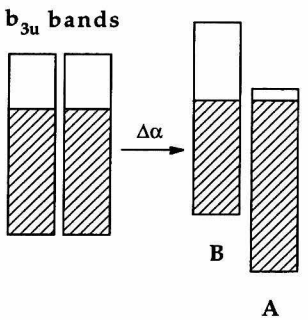

11

P_4 rings in the 3D structure. In second place, as a result of the unit cell doubling, each of the b_{3u} bands (b_{3u} and b'_{3u}, **6**) is doubled giving rise to two branches. The lowest levels of these bands ($1b_{3u}$ and $1b'_{3u}$ at Γ, Fig. 9) are built up from in-phase combinations of the b_{3u} framework orbitals of one Ni_2P_2 ring in each of the two chains and are allowed by symmetry to mix with the π-bonding orbitals of the perpendicular Ni_2P_2 rings (**8a**). The highest levels ($2b_{3u}$ and $2b'_{3u}$ at Γ, Fig. 9) are out-of-phase combinations (**8b**) and mix with π* orbitals of the alternate rings. Finally, at the Z point the framework orbitals mix with π non-bonding orbitals (**9**), and the two branches are degenerate, resulting in the overall *folded* band aspect [9]. The partial filling of these bands can be roughly represented by an $(a_g)^2(b_{2g})^2(b_{3u})^{1.2}(b_{1u})^{1.8}$ configuration (the numbers given are only for the purpose of illustration and should not be taken in a numerical sense) for the framework orbitals, consistent with the relatively long experimental through-ring Ni···Ni distance of 2.89 Å.

In the α-$BaNi_2P_4$ to β-$BaNi_2P_4$ phase transition, two different Ni_2P_2 rings result, one with short, another one with long Ni···Ni distance, labelled as **A** and **B** (**10**), respectively. Upon distortion, the band structure is modified (Fig. 8b), but no gap appears at the Fermi level. This result indicates that the distortion cannot be attributed to a Peierls effect, a result that could be anticipated from the strong three-dimensional character of the undistorted structure. The most salient changes in the band structure appear along the ΓZ direction close to the Fermi level, where the b_{3u} bands loose their degeneracy and are split in energy.

The effect of distortion **10** on the b_{1u} and b_{3u} bands along the ΓZ line is shown in Fig. 9, where the splitting of the b_{3u} set at $\Delta\alpha$ = 20° can be clearly appreciated. One of the two b_{3u} bands becomes mostly localized at the **A** rings (**10**), and is stabilized due to its σ*(P···P) and π(Ni···Ni) properties. The other band, localized at the **B** rings (**10**) is destabilized. The overall effect is schematically shown in the block diagram **11**. As a result, the band centered on rings **A** increases its population upon distortion, whereas the one centered on rings **B** is partially depopulated. The differences in electron population between the two types of Ni_2P_2 rings can be seen in the calculated charge for the corresponding P atoms (Table 3). An indirect result of all this is that the Fermi level is lowered and the population of the b_{1u} band also decreases. Although we have seen above that it is not appropriate to talk in terms of integer FEC numbers in the present case, one can clearly identify a trend towards a configuration of the type $(a_g)^2(b_{2g})^2(b_{3u})^{1.8}(b_{1u})^{1.6}$ for the **A** rings and

$(a_g)^2(b_{2g})^2(b_{3u})^1(b_{1u})^{1.6}$ for the **B** rings, if the 3D structure were severely distorted. Notice that the Ni···Ni distances in both rings (2.77 and 3.02 Å for rings **A** and **B**, respectively) are still relatively long, compared with those in binuclear complexes of tetrahedrally coordinated Ni with phosphido bridges with a FEC of 6 (2.50- 2.56 Å) [10-13].

A consequence of the electron transfer from rings **B** to **A** is that the overall population of the framework bonding orbitals decreases upon distortion for **B** and increases for **A**. Hence, the Ni-P bonds are slightly but significantly longer in the **B** rings (2.240(2) Å) than the corresponding bonds in **A** (2.219(2) Å). All the trends in bond distances are nicely followed by the calculated interatomic overlap populations (Table 3).

Conclusions

In this work we have analyzed the electronic structure of the recently synthesized $BaNi_2P_4$ compound, in an attempt to understand the complicated bonding relations that hold together a complex 3D net of nickel and phosphorus rings. Special attention has been devoted to the experimentally detected phase transition that this compound undergoes at approximately 100°C.

Our results indicate that the basic structure of the $(Ni_2P_4)^{2-}$ subnet found in this compound can be rationalized by using a simple molecular model and applying the recently proposed framework electron counting rules. These qualitative rules can be applied consistently to the Ni_2P_2 rings found in both the high and low temperature structures of $BaNi_2P_4$. Different through-ring Ni···Ni distances in the two non-equivalent Ni_2P_2 rings found in the low temperature β-$BaNi_2P_4$ phase can be rationalized from the filling of the framework bonding bands.

Although a simple 1D model suggests the appealing hypothesis of a Peierls distortion as the origin of the phase transition in this compound, a careful examination of the electronic structure of $BaNi_2P_4$ makes it clear that the Peierls distortion mechanism is not responsible for the observed deformation. Instead, $BaNi_2P_4$ is predicted to be a 3D metal in both its high and low temperature phases. The driving force for the distortion cannot be explained at the one-electron level of theory, although the difference in the calculated energies for both phases is small. Hence, two-electron effects or entropic factors might be at the origin of the phase transition.

Acknowledgements A. A. P. thanks the Ministerio de Educación y Ciencia for a doctoral fellowship and for a grant that made her stay at Cornell University possible. Financial suport for this work was provided by DGES through grant number PB95-0848-C02-01. The authors are grateful to E. Canadell for clarifying discussions on the possible existence of a Peierls distortion in $BaNi_2P_4$.

Appendix

Computational details

All the molecular orbital calculations were of the extended Hückel type [14, 15] and all band structure calculations presented in this work were obtained by using the extended Hückel tight-binding method [15-17]. The off-diagonal elements of the Hamiltonian matrix were evaluated with the modified Wolfsberg-Helmholz formula [18]. Extended Hückel computations were performed using the YAeHMOP package [19]. The atomic parameters used in this calculations are shown in Table 4. The geometries adopted for the model compounds were as follows: PH_3 groups were used for the molecular model as terminal ligands, with Ni-P = 2.227 Å and P-H = 1.350 Å and with tetrahedral angles. The bridging groups PH_2 were used with Ni-P = 2.227 Å (experimental value for α-$BaNi_2P_4$) and P-H = 1.350 Å, and were oriented preserving a D_{2h} symmetry for the Ni_2P_2 core for the molecule and chain models, with H-P-H = 109.5 degrees.

References

1. Keimes J, Johrendt D, Mewis A (1995) Z Anorg Allg Chem 621:925-930
2. Johrendt D, Mewis A (1994) J Alloys Comp 205:183-189
3. Jung D, Whangbo M-H, Alvarez S (1990) Inorg Chem 29:2252-2255
4. Llunell M, Alemany P, Alvarez S, Zhukov VP, Vernes A (1996) Phys Rev B 53:10605-10609
5. Alemany P, Alvarez S (1992) Inorg Chem 31:4266-4275
6. Aullón G, Alemany P, Alvarez S (1994) J Organomet Chem 478:75-82
7. Silvestre J, Hoffmann R (1985) Inorg Chem 24:4108-4119
8. Peierls RE (1955) Quantum Theory of Solids. Oxford University Press, London
9. Hoffmann R (1988) Solids and Surfaces: A Chemist's View of Bonding in Extended Structures, VCH, New York, and references therein
10. Jarvis JAJ, Mais RHB, Owston PG, Thompson DT (1970) J Chem Soc A:1867-1872
11. Jones RA, Norman NC, Seeberger MH, Atwood JL, Hunter WE (1983) Organometallics 2:1629-1634
12. Barnett BL, Kruger C (1973) Cryst Struct Commun 2:85-88
13. Arif AM, Jones RA, Schwab ST (1987) J Coord Chem 16:51-57
14. Hoffmann R, Lipscomb WN (1962) J Chem Phys 36:3489-3493
15. Hoffmann R (1963) J Chem Phys 39:1397-1412
16. Whangbo M-H, Hoffmann R (1978) J Am Chem Soc 100:6093-6098
17. Whangbo M-H, Hoffmann R, Woodward RB (1979) Proc R Soc London, A 366:23-46
18. Ammeter JH, Bürgi H-B, Thibeault JC, Hoffmann R (1978) J Am Chem Soc 100:3686-3692
19. Landrum G (1995) YAeHMOP - Yet Another extended Hückel Molecular Orbital Package (Version 1.2), Cornell University, Ithaca, NY
20. Lauher JW, Elian M, Summerville RH, Hoffmann R (1976) J Am Chem Soc 98:3219-3224
21. Llunell M, Alvarez S, Alemany P, Hoffmann R (1996) Inorg Chem 35:4683-4689
22. Vela A, Gázquez JL (1988) J Phys Chem 92:5688-5693
23. McLean AD (1981) Atomic Data Nucl Data Tables 26:209